

# Digital Low-Level RF control system for Accumulator Ring at Advanced Light Source Upgrade Project

Qiang Du\*, Shreeharshini Murthy, Michael Betz, Kevin Bender, Wayne Lewis, Najm Us Saqib, Sergio Paiagua, Lawrence Doolittle, Carlos Serrano, Benjamin Flugstad, Kenneth Baptiste

Lawrence Berkeley National Laboratory  
1 Cyclotron Rd, Berkeley, CA, 94720 USA  
Email: QDu@lbl.gov

arXiv:2210.05095v1 [physics.acc-ph] 11 Oct 2022

**Abstract**—Currently ALS is undergoing an upgrade to ALS-U to produce 100 times brighter soft X-ray light. The LLRF system for Accumulator Ring (AR) is composed of two identical LLRF stations, for driving RF amplifiers. The closed loop RF amplitude and phase stability is measured as  $< 0.1\%$  and  $< 0.1^\circ$  respectively, using the non-IQ digital down conversion together with analog up/down conversion, under a system-on-chip architecture. Realtime interlock system is implemented with  $< 2\mu s$  latency, for machine protection against arc flash and unexpected RF power. Control interfaces are developed to enable PLC-FPGA-EPICS communication to support operation, timing, cavity tuning, and interlock systems. The LLRF system handles alignment of buckets to swap beams between AR and Storage Ring by synchronous phase loop ramping between the two cavities. The system also includes an optimization routine to characterize the loop dynamics and determine optimal operating point using a built-in network analyzer feature. A cavity emulator of 31 kHz bandwidth is integrated with the LLRF system to validate the performance of the overall system being developed.

## I. INTRODUCTION

The Advanced Light Source (ALS) at Lawrence Berkeley National Laboratory is a U.S. Department of Energy’s synchrotron light source user facility that is operational since 1993. With circumference of 196.8 m, the ALS Storage Ring (SR) keeps electron beam current of 500 mA at 1.9 GeV under multi-bunch mode user operation to deliver synchrotron X-rays to surrounding 40 experimental end stations. [1]

There is an ongoing ALS upgrade project (ALS-U), scheduled to upgrade towards 2 orders of magnitude increase in brightness and flux of 1keV soft X-rays at diffraction limit. The ALS-U project involves a new 2.0 GeV Storage Ring (SR) in existing tunnel optimized for low emittance, and add a new 2.0 GeV Accumulator Ring (AR) for full energy swap-out injection and bunch train recovery, as shown in Fig. 1. The AR is a triple-bend-achromat (TBA) lattice, very similar to the current ALS SR lattice. The RF system requirements for the TBA lattice can be found in Table I. Two normal conducting RF cavities have been selected for AR. Each RF cavity is driven by an identical chain from a high power solid-state amplifier (SSA) and low-level RF (LLRF) control system, together with personnel safety interlocks, equipment protection interlocks, etc.

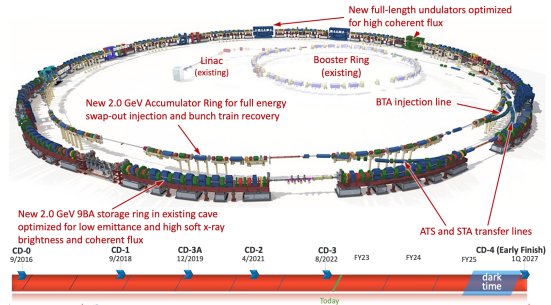


Fig. 1: ALS Upgrade with both Accumulator and Storage Rings

	ALS SR	ALS-U SR	ALS-U AR	
Cavity RF Frequency	499.64	500.394	500.394	MHz
Number of Cavities	2	2	2	
$\frac{R}{Q}$ (ea)	4.9	4.9	3.4-3.5	MΩ
Cavity voltage	671	300	500	kV
$\beta$	2.9	10.6	1.18	
Energy loss per turn	329	347	270	keV
BM Beam Power	141	125	13.3	kW
ID Beam Power	42	35		kW
3HC Beam Power	7.3	13.8		kW
Parasitic Beam Power	2.9 (est.)	2.6 (est.)	0.2	kW
Total Beam Power	192.9	176.4	13.5	kW
Cavity Power(no beam)	46	9.2	36.0	kW
Cavity Power(beam)	142.5	97.4	42.7	kW
High Power Amplifier	294.0	197.5	60	kW

TABLE I: ALS and ALS-U AR and SR RF parameters

## II. HARDWARE DESIGN

The AR LLRF system consists of two identical stations, each controlling one SSA and RF cavity, but sharing communication interface with a central interlock PLC and both stations are coordinated by common timing events for synchronous operations. Each LLRF station consists of an analog frontend chassis and a digital chassis. The analog chassis receives ALS-U master oscillator and generates local oscillator (LO) signal, and provides frequency conversions including 6 channels of down-conversion and 2 channels of up-conversion between

RF and IF frequencies, following the non-IQ down-conversion configuration:

$$\begin{aligned}
 f_{MO} &= 500.39 \text{ MHz} \\
 f_{LO} &= \frac{11}{12} f_{MO} = 458.69 \text{ MHz} \\
 f_{IF} &= \frac{1}{12} f_{MO} = 41.69 \text{ MHz} \\
 f_{\text{Sample}} &= \frac{1}{4} f_{LO} = 114.67 \text{ MHz} \\
 \frac{f_{IF}}{f_{\text{Sample}}} &= \frac{4}{11} = \theta \simeq 130.9^\circ
 \end{aligned}$$

The analog frontend chassis assembly is shown as in Fig. 2. The up-down-conversion PCB boards are existing designs from Jefferson Lab with 500 MHz center frequency, featured with high channel isolation, programmable TX attenuation, RF switch and various diagnostics and monitoring points. The LO generation PCB board uses single side band modulation to generate four  $f_{LO}$  signals that feed into up-down-conversion boards, and the digital chassis for sampling clock.

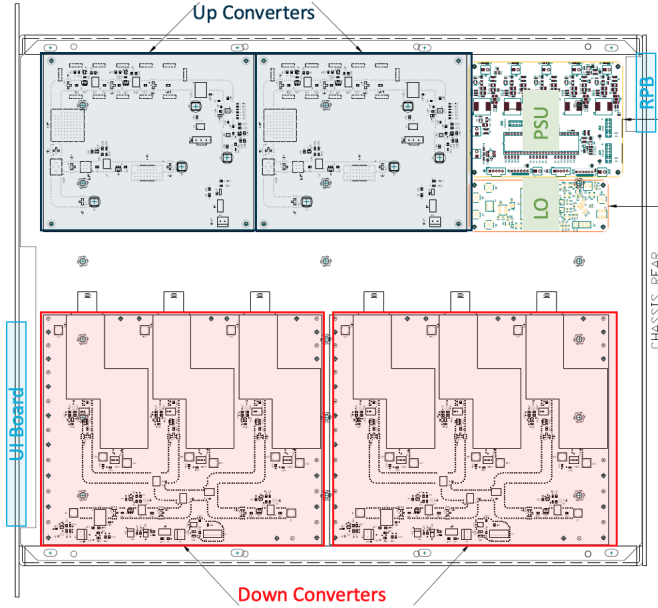


Fig. 2: Analog frontend chassis: 6 down + 2 up conversion, LO generation

There is a centralized power supply controller board that is responsible for configuration of LO board, continuous monitoring and interlocking of the LO level, temperature, voltage and current consumptions, and provide an interactive local user interface through an OLED display. Remote control is available through an RS485 port with Modbus RTU protocol.

The digital chassis consists a Marble-Mini [2] FPGA carrier board and a Zest digitizer board [3], as shown in Fig. 3. Both boards are available through CERN Open Hardware License (OHL v1.2). The  $f_{LO}$  signal is feed into the clock input of Zest board for generation and distribution of  $f_{\text{Sample}}$  to two 16-bit, four channel ADC with sampling rate up to

125 MHz (AD9653), and one 16-bit, dual channel DAC with sampling rate up to 250 MHz (AD9781). The Zest board is used in LCLS-II LLRF project with superior low noise and channel crosstalk performances. The Marble family FPGA carrier boards are used in many other projects in ALS and PIP-II LLRF control.

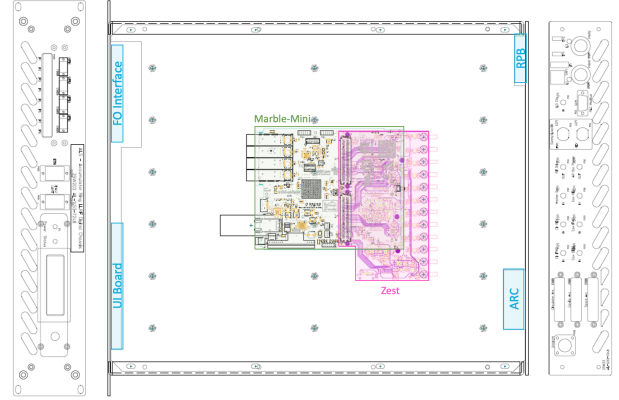


Fig. 3: Digital chassis: Marble-Mini FPGA carrier and Zest digitizer

For ALS-U AR LLRF control, the 6 down-converted IF signals are fed from the analog frontend chassis for operation, including cavity probe, cavity forward and reverse, and circulator load forward and reverse signals. The 2 additional ADCs in Zest board are used to directly sampling the test load signals for high power RF system commissioning.

### III. FIRMWARE DESIGN

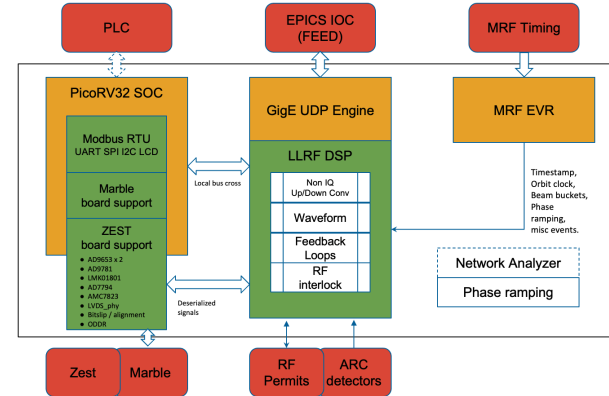


Fig. 4: Digital Chassis Firmware architecture

Fig. 4 shows the digital chassis firmware architecture, which is built on top of BSD licensed open source LLRF library Bedrock [4]. We use an open source, size optimized RISC-V CPU PicoRV32 [5] to handle system configuration, boot-time self checking, continuous status monitoring, and remote interfacing with PLC systems via the RS485 / Modbus RTU port which is similar to the analog frontend chassis. The footprint of the firmware is only 24 kB of RAM and 750–2000 LUTs. At the same time, we use BerkeleyLab’s realtime

Ethernet fabric infrastructure packet badger to provide a UDP communication as another local bus master, which has the priority to directly access DSP registers for realtime EPICS applications, including configurable waveforms for any RF signals.

The feedback DSP core is implemented as shown in Fig. 5. A classical non-IQ digital down conversion algorithm [6] is implemented to digitally down-convert the IF signals and reconstruct their IQ values using a local direct digital synthesizer (DDS): Given  $\frac{f_{IF}}{f_{Sample}} = \frac{4}{11} = \theta \simeq 130.9^\circ$ ,

$$\begin{pmatrix} y_n \\ y_{n+1} \end{pmatrix} = \begin{pmatrix} \cos(n\theta) & \sin(n\theta) \\ \cos((n+1)\theta) & \sin((n+1)\theta) \end{pmatrix} \begin{pmatrix} I \\ Q \end{pmatrix}$$

$$\begin{pmatrix} I \\ Q \end{pmatrix} = \frac{1}{\sin \theta} \begin{pmatrix} \sin((n+1)\theta) & -\sin(n\theta) \\ -\cos((n+1)\theta) & \cos(n\theta) \end{pmatrix} \begin{pmatrix} y_n \\ y_{n+1} \end{pmatrix}$$

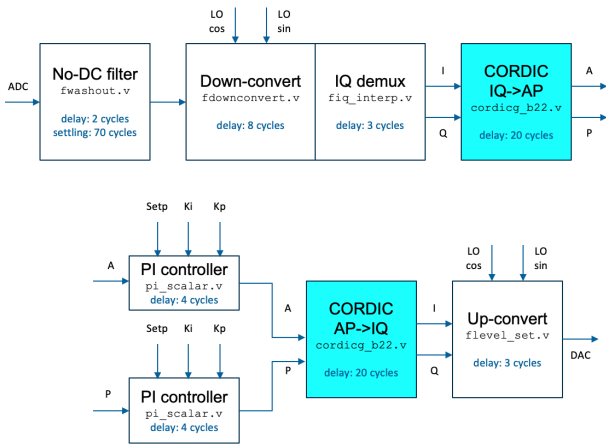


Fig. 5: Feedback DSP core firmware implementation in fabric

The total latency of the feedback DSP core is 50 clock cycles or 436 ns. In parallel, all signals are passed to a multichannel RF waveform buffer with configuration decimation and cascaded integral-comb (CIC) filter, where a fixed scaling waveform branches off for realtime RF power interlocking and machine protection purpose, as shown in Fig. 6. The fast RF power interlock has a configurable mode of comparison between the measured RF amplitude and a pair of programmable thresholds for disabling the DAC output in case of unexpected RF power or phase measurements, within  $< 1\mu s$  limit to protect down stream high power amplifiers and equipments.

There are two Proportional-Integral (PI) controllers that are responsible for the feedback loop control of cavity probe signal's amplitude and phase respectively. A classical, scalar PI controller with slew rate limiter and phase wrapping capability is implemented as shown in Fig. 7 with simple transfer function:

$$C(z) = K_p + K_i \frac{1}{1 - z^{-1}}, \quad T = \frac{1}{f_{clk}}$$

We also implemented a state-machine that can synchronously rotate the phase loop setpoints of both LLRF

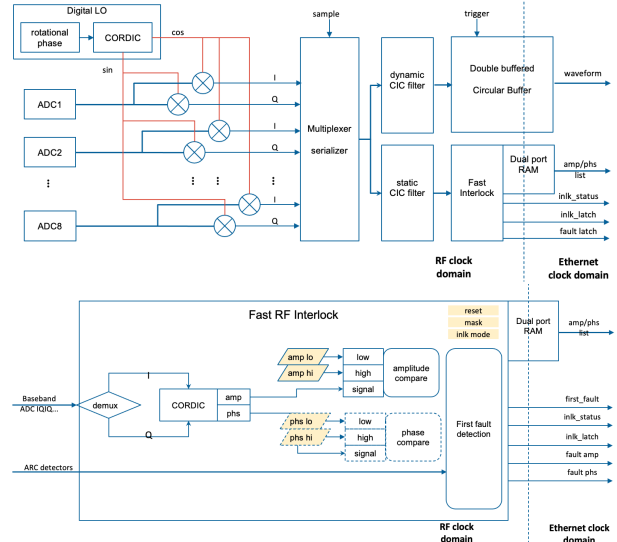


Fig. 6: Multichannel RF waveforms and configurable interlock

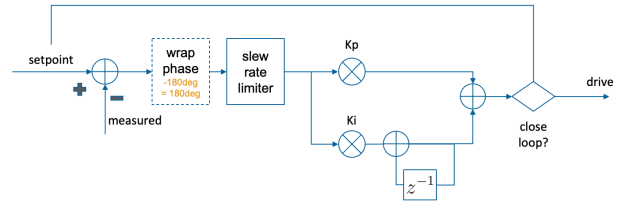


Fig. 7: PI controller

stations, so that the relative RF bucket can be aligned between AR and SR. This is required for beam swapping operation for ALS-U. This *phase ramping* procedure is repeatably triggered by a common timing event with delay configuration and fault handling.

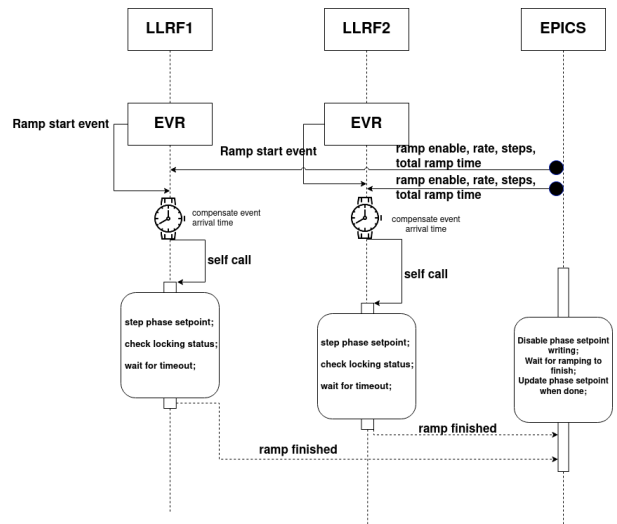


Fig. 8: Bucket alignment scheme between AR and SR

#### IV. SOFTWARE

Both LLRF stations are managed by a center master interlock PLC through RS485 / Modbus RTU links. The PLC continuously polling registers through the interrupt service function of the PicoRV32 CPU, which handles Modbus RTU protocol and retrieves realtime register information for monitoring.

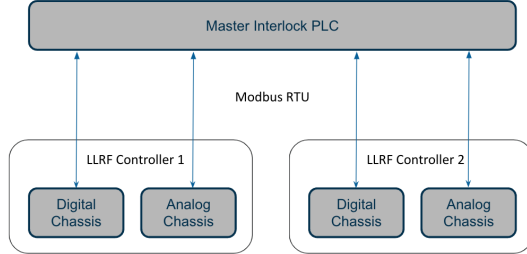


Fig. 9: PLC-FPGA interfaces

PLC screens are developed for configuration of operation parameters including RF power / ARC interlock mode and thresholds.

An EPICS IOC is built based on single-source-of-truth register mapping, sharing the same architecture with LCLS-II LLRF project. An example of a working Phoebus engineering screen is shown in Fig. 10

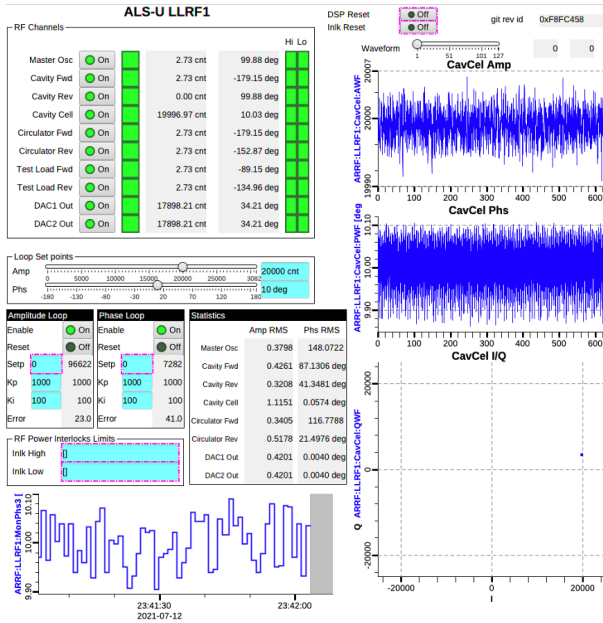


Fig. 10: Example Phoebus GUI

#### V. PERFORMANCE

The single side band  $f_{LO}$  generation has  $> 90$  dB spurious free dynamic range (SFDR), with  $-84.6$  dB MO carrier feedthrough. The measured additive phase noise of LO signal is 29 fs [1Hz, 1MHz]. The measured RF drive signal also has  $> 95$  dB SFDR, with RMS phase noise of 30 fs [1Hz, 1MHz].

LO Spurious Free Dynamic Range	$> 90$	dB
Carrier feedthrough in LO signal	$-84.6$	dB
RMS Additive LO phase jitter [1Hz, 1MHz]	29	fs

TABLE II: Single Side Band LO generation benchmark

TX Spurious Free Dynamic Range	$> 95$	dB
RMS Additive phase jitter [1Hz, 1MHz]	30	fs

TABLE III: RF drive signal (after up-conversion) benchmark

The measured receiver channel-to-channel isolation is  $> 86$  dB as shown in Fig. 11.

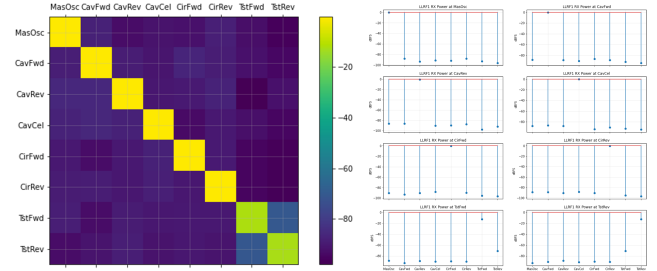


Fig. 11: Receiver channel-to-channel isolation

The measured RF-to-RF group delay is  $< 1\mu$  second by directly looping back RF drive signal and one of the receiving signals, when pulsing the drive signal, as shown in Fig. 12.

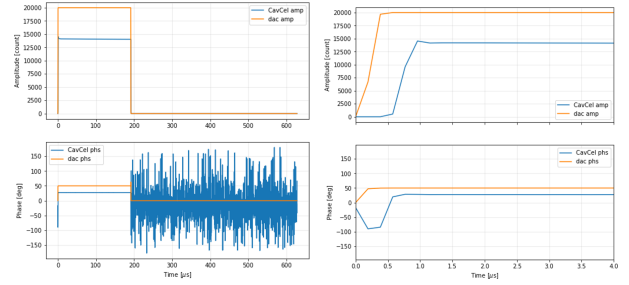


Fig. 12: Group Delay measurement

The feedback loop noise floor is measured also by looping back TX and RX (cavity probe signal), and using the spectrum analysis of the waveforms. We used an external RF signal analyzer (R&S FSWP) and measured that the out-of-the-loop RMS amplitude stability is  $< 0.005\%$ , and RMS phase loop stability is  $< 0.008^\circ$ .

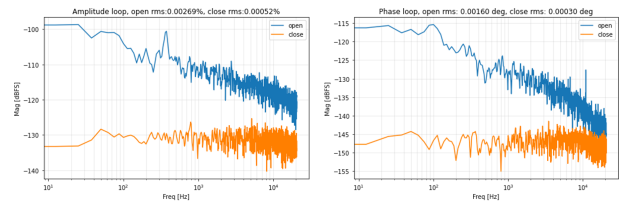


Fig. 13: In-loop stability measurement

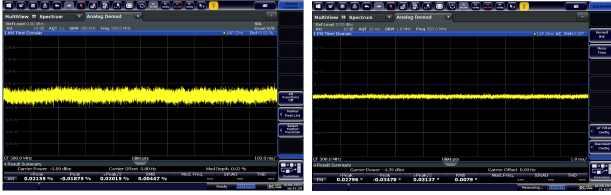


Fig. 14: Out-of-loop stability measurement

We also measured the frequency response of both loops when directly looped back, by adding a known excitation frequency on the setpoint of either amplitude or phase loop, and analysis the response spectrum. The resulting Bode plot is shown in Fig. 15.

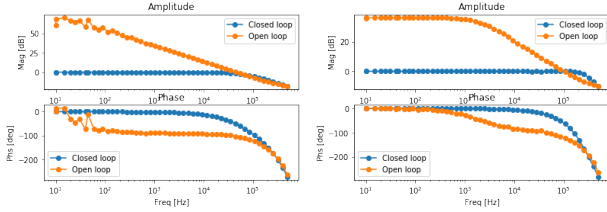


Fig. 15: Bode plot of both loops when directly looped back

The *phase ramping* bucket alignment test result is shown in Fig. 16. This is done by ramping of phase setpoint from A to B, at a configurable speed, when the loop is closed. The ramping successfully executed greater than 7 period of RF cycle, after being triggered by an timing event, which is required by beam swapping operation between AR and SR.

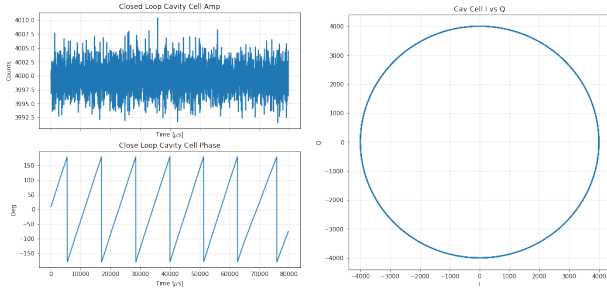


Fig. 16: Phase ramping process when both loops are closed

## VI. CONCLUSION

The ALS-U AR LLRF system is developed and tested on the bench, where its performance meets the requirements. The design is conducted using fully open source hardware, firmware and software libraries offered by BerkeleyLab. The same design is also tested in Brazilian Light Source (SIRIUS) at a different frequency configuration, where  $f_{LO} = \frac{23}{34} f_{MO} = 479.17 \text{ MHz}$  and  $\frac{f_{IF}}{f_{Sample}} = \frac{4}{23}$ . The system is ready for cavity test and commissioning at ALS-U project.

## ACKNOWLEDGMENT

This work is supported by the Office of Science, Office of Basic Energy Sciences, of the U.S. Department of Energy under Contract No. DE-AC02-05CH11231.

## REFERENCES

- [1] Q. Du, L. Doolittle, M. Betz, M. Vinco, and K. Baptiste, “Digital low-level rf control system for advance source storage ring,” in *Low Level RF workshop 2019, Chicago, IL, USA, Sept 29 – Oct 3, 2019*, 2019.
- [2] “Marble-Mini board: Dual FMC NAD/AMC FPGA Carrier,” <https://github.com/BerkeleyLab/Marble-Mini>, 2019.
- [3] “Zest board: Dual FMC ADC and DAC digitizer,” <https://github.com/BerkeleyLab/Zest>, 2019.
- [4] “Bedrock: Open Source LLRF FPGA Firmware Library,” <https://github.com/BerkeleyLab/Bedrock>, 2019.
- [5] “PicoRV32 – A Size-Optimized RISC-V CPU,” <https://github.com/cliffordwolf/picorv32>, 2015.
- [6] L. Doolittle, H. Ma, and M. S. Champion, “Digital Low-Level RF Control using Non-IQ Sampling,” in *Proceedings of LINAC 2006, Knoxville, Tennessee USA*. Citeseer, 2006, pp. 568–570.